JOURNAL OF SOLID STATE CHEMISTRY **126,** 177–183 (1996)
ARTICLE NO. 0326

Calzirtite after Tetragonal ZrO_2 Studied by Transmission Electron Microscope

Jing-Shi Lin and Pouyan Shen[1]

Institute of Materials Science and Engineering, National Sun Yat-sen University, Kaohsiung, Taiwan 804

Received January 17, 1996; in revised form June 26, 1996; accepted July 2, 1996

Reactive sintering of CaO, ZrO_2, and TiO_2 (2:5:2 in molar ratio) powders at 1320°C for 2 weeks caused the topotaxial formation of calzirtite ($Ca_2Zr_5Ti_2O_{16}$, a 3 × 3 × 2 fluorite superstructure denoted as czt) after ZrO_2 nuclei, presumably of tetragonal (t-) symmetry with an orientational relationship $[100]_t//[100]_{czt}$; $[001]_t//[001]_{czt}$. To maintain a t-ZrO_2 precursor for the subsequent calzirtite formation, it was essential to have Ti^{4+} dissolved faster than Ca^{2+} in the ZrO_2 lattice. The calzirtite grains thus formed have no twin variants but have ordered domains and a new supercell which can be indexed as an 6 × 3 × 4 array of the fluorite subcell, due to ordering of two closely spaced *M*(1) positions (0.93Ti + 0.07Zr, determined by Rossell). The 6 × 3 × 4 supercell appeared as disk-like variants in the calzirtite matrix. © 1996 Academic Press, Inc.

1. INTRODUCTION

The fluorite-related phases in the system $CaO–ZrO_2–TiO_2$ have attracted interest as high-level radioactive waste immobilizers and as potential solid electrolytes (1–5). Calzirtite ($Ca_2Zr_5Ti_2O_{16}$, czt), being a fluorite superstructure (3 × 3 × 2 array of the fluorite subcell) with the space group $I4_1/acd$ (6), is expected to have a topotaxial lattice relationship with the cubic (c-) ZrO_2 nuclei, an isostructure of fluorite. Indeed, the c-ZrO_2 either in the form of particles or as a matrix phase in partially stabilized zirconia (PSZ, i.e., c-ZrO_2 with tetragonal (t-) ZrO_2 precipitates) can act as topotaxial nuclei of calzirtite phase (7). The calzirtite thus formed has transformation twin variants because any one of the principal axes of the c-ZrO_2 can become the *c*-axis of the calzirtite phase. From the crystallographical point of view, a superstructure is a subgroup of its parent phase and can be formed by substitutional derivation (8). Since calzirtite is a subgroup of t-ZrO_2 (space group $P4_2/nmc$ (9)), it is expected to nucleate also from t-ZrO_2.

This study intended to show that twin-free calzirtite can indeed be derived from ZrO_2 by reactive sintering the constituent oxides at 1320°C for 2 weeks in an open air furnace because the ZrO_2 nuclei became t- rather than c-symmetry under such a condition. We report also the discovery of a superlattice of calzirtite by electron diffraction which sheds light on the extent of cation ordering, a controversy in the literature (6).

2. EXPERIMENTAL

Reagent grade $CaCO_3$ (Showa), ZrO_2 (Gredmann, monoclinic (m-) symmetry), and TiO_2 (Cerac) powders in a molar ratio of 2:5:2 (designated as $C_2Z_5T_2$) were ball (PSZ) milled in distilled water for 24 h, oven dried, and calcined at 900°C for 4 h in an alumina crucible to form an intimate mixture of the oxide powders. The $C_2Z_5T_2$ batch was die pressed (100 MPa) as disks 10 mm in diameter, put in a platinum crucible, and then fired at 1320°C for 2 weeks followed by cooling in an open air furnace to form calzirtite pellets. The fired pellets contain almost pure calzirtite phase according to X-ray diffraction (Cu$K\alpha$, 35 kV, 25 mA).

The microstructures of sintered calzirtite polycrystals were studied by transmission electron microscopy (TEM, using JEOL 200 CX at 200 kV and JEOL JSM3010 at 300 kV). TEM sample foils were prepared by dimple grinding the thin sections followed by Ar-ion milling to electron transparency. The bright field image (BFI), dark field image (DFI), and selected area diffraction (SAD) patterns were used to study the microstructures of calzirtite and its supercell.

3. RESULTS

The calzirtite polycrystals thus prepared were ca. 2 to 3 μm in size and faceted due to solid-state sintering as shown by the TEM image (Fig. 1). The individual grains were found to have a single variant of calzirtite and a new supercell of calzirtite following a parallel crystallographic

[1] To whom correspondence should be addressed.

0022-4596/96 $18.00

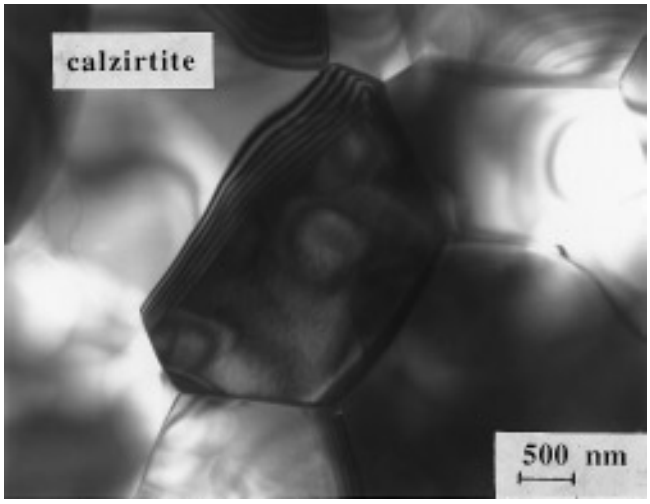

FIG. 1. BFI of calzirtite polycrystals prepared by reactive sintering of the constituent oxides at 1320°C for 2 weeks.

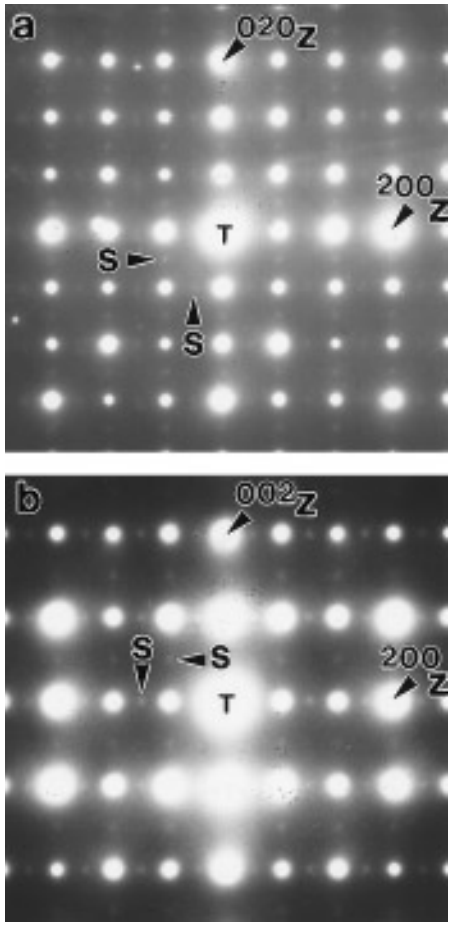

FIG. 2. SAD patterns showing a single variant of calzirtite derived from ZrO_2 and weak extra spots due to the $6 \times 3 \times 4$ supercell: (a) [001] and (b) [010] zone axes, the fundamental spots are indexed according to fluorite subcell and two variants of the $6 \times 3 \times 4$ supercell (arrows) can be recognized in (a). Z and S denotes zirconia and supercell, respectively.

relationship with respect to calzirtite as indicated by the SAD patterns in the [001] and [010] zone axes (Figs. 2a and 2b, respectively, the schematic indexing refers to Fig. 3). The $(1\bar{1}2)$ spot of zirconia appeared in the $[\bar{1}11]$ zone axis (Fig. 4), suggesting the presence of the t-ZrO_2 phase although it cannot be discerned clearly from the DFI due to the limitation of the aperture size and the weak intensity of the spot. The lattice correspondence must be $[100]_t // [100]_{czt}$; $[001]_t // [001]_{czt}$ in order to form twin-free calzirtite from t-ZrO_2. The schematic indexing of the reciprocal lattice (Fig. 5) based on the SAD patterns depicts a possible $6 \times 3 \times 4$ array of the fluorite subcell. Two variants of the $6 \times 3 \times 4$ supercell are allowed from the crystallographic point of view and were indeed observed (Fig. 2a).

The calzirtite grain consists of domains which are visible with the (440) spot of calzirtite (Fig. 6a) but invisible with the (220) reflection of the t-ZrO_2 subcell (Fig. 6b), suggesting that they are an anti-phase boundary (APB) due to ordering. Occasionally, dislocation arrays were found at the APB (Fig. 7).

The $6 \times 3 \times 4$ phase was uniformly distributed in the calzirtite grains as indicated by the DFI analyses. For example, the {332} spot of calzirtite is superimposed with the fundamental {111} spot of zirconia but not with the $6 \times 3 \times 4$ superlattice spot (refer to Fig. 5). Thus, the DFIs using the {332} spot of calzirtite showed the $6 \times 3 \times 4$ phase in dark areas (Fig. 8); whereas a $6 \times 3 \times 4$ spot not

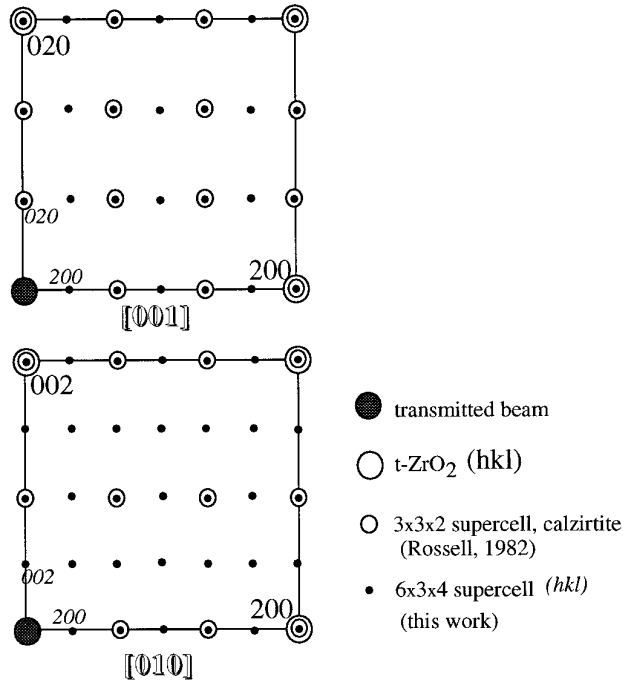

FIG. 3. Schematic drawing of SAD patterns in Fig. 2. Only one variant of the $6 \times 3 \times 4$ supercell is indexed.

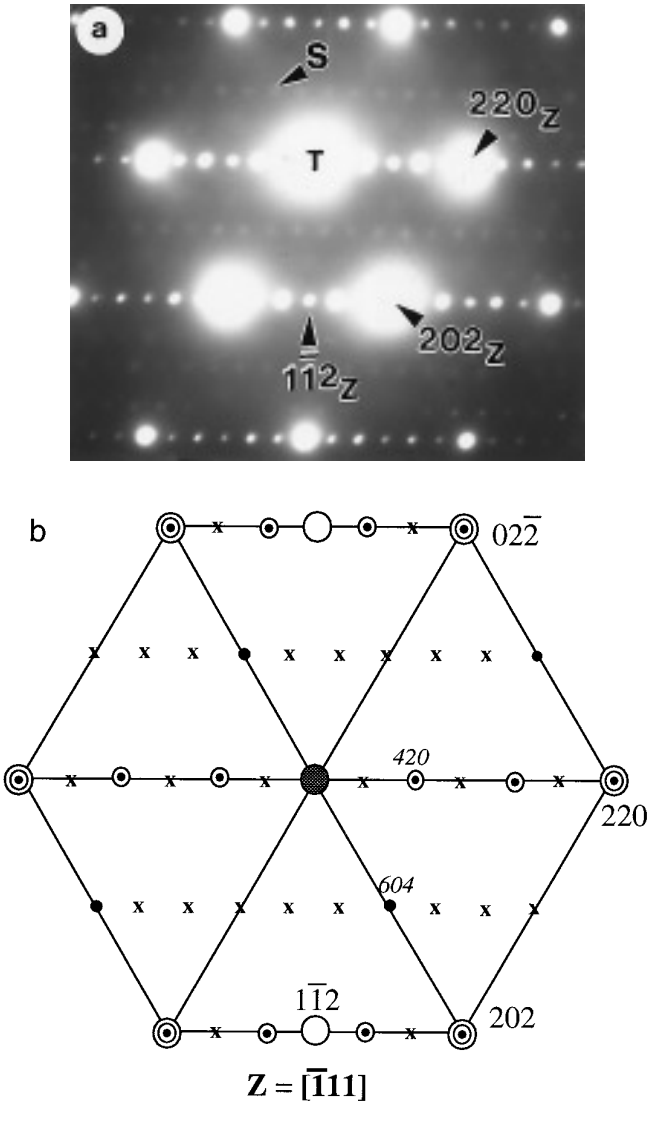

FIG. 4. (a) SAD pattern of calzirtite grain in the [$\bar{1}$11] zone axis showing diffraction spots of t-ZrO_2 subcell and its $3 \times 3 \times 2$ supercell (i.e., calzirtite). The weak extra spots are due to a $6 \times 3 \times 4$ supercell and double diffraction. (b) Schematic indexing of the [$\bar{1}$11] SAD pattern. Note ($1\bar{1}2$) spot is due to t- rather than c-ZrO_2 phase.

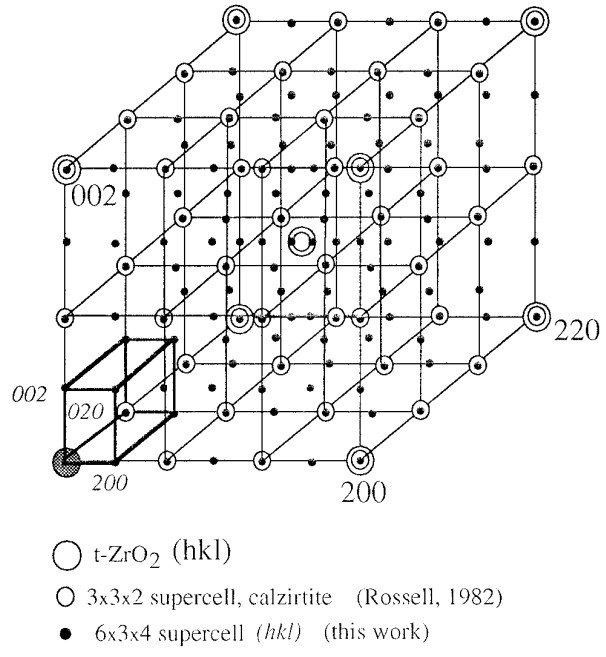

FIG. 5. Schematic drawing of the reciprocal lattice of t-ZrO_2 and its derivatives based on the SAD patterns in Figs. 2 and 4. The edges of a $6 \times 3 \times 4$ supercell are depicted in bold lines.

superimposed with the calzirtite spot shows the $6 \times 3 \times 4$ phase in bright areas (Fig. 9). Occasionally the $6 \times 3 \times 4$ phase had a larger size and formed disk-like variants (Fig. 10). In general, the $6 \times 3 \times 4$ disk is coherent with respect to the calzirtite matrix as indicated by the lattice image (Fig. 11).

4. DISCUSSION

4.1. Phase Transformation of ZrO_2 upon Reactive Sintering

The absence of twin variants in the calzirtite grain suggests that its precursor remained as t-ZrO_2, rather than c-ZrO_2 phase and/or (c + t)-ZrO_2 assemblages, the known precedents of twinned calzirtite (7). In fact, the t-ZrO_2 spot ($1\bar{1}2$) was indeed observed in the present sample (Fig. 4). (More evidence of the nucleation of calzirtite on t-ZrO_2 may be obtained by the examination of partially reacted materials which contain the precipitate and substrate.) This t-ZrO_2 nuclei must be derived from the starting m-ZrO_2 powder upon reactive sintering of the CaO, ZrO_2, and TiO_2 powders at 1320°C, because the m → t transformation temperature of pure ZrO_2 is ca. 1100–1200°C (10). To maintain a t-ZrO_2 phase during reactive sintering, it was essential to have Ti^{4+} dissolved faster than Ca^{2+} in the ZrO_2 lattice as discussed below.

The dissolution of Ti^{+4} has been well established to lower the martensitic t → m transformation temperature (M_s) of ZrO_2, i.e., stabilize t-ZrO_2, but not c-ZrO_2 or (c + t)-ZrO_2 (11). (Only under reduced oxygen pressure, the divalent cation of Ti can be significant enough to form (c + t)-ZrO_2, i.e., Ti–PSZ (12), due to the effect of electric charge compensating oxygen vacancies analogous to the case of other PSZ's including Ca–PSZ (13).) It is noteworthy that

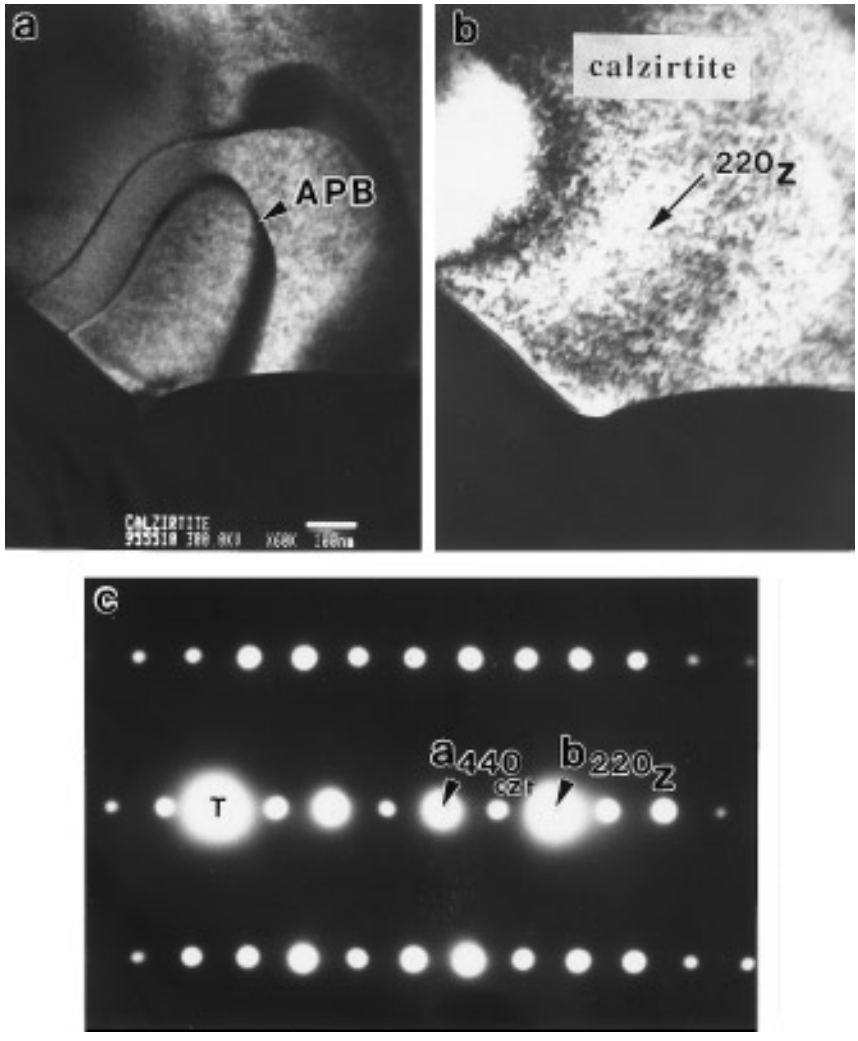

FIG. 6. APB of calzirtite: (a) visible using (440) spot of calzirtite; (b) invisible using (220) spot of t-ZrO_2 subcell; (c) corresponding SAD pattern.

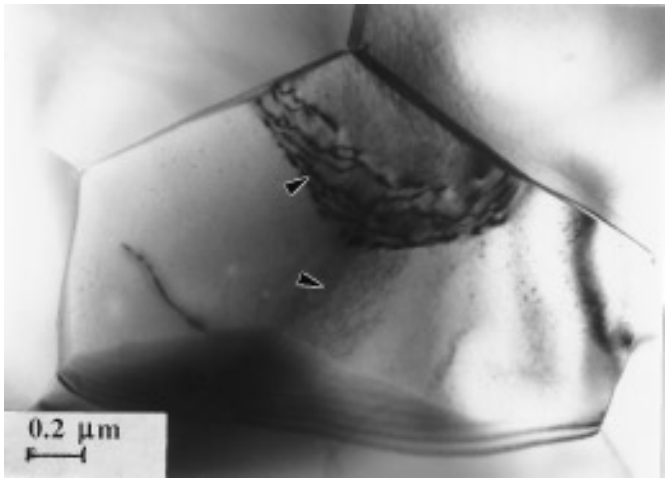

FIG. 7. BFI of dislocation arrays in calzirtite grain.

(Ca,Ti)–PSZ can still be fabricated in the ZrO_2 rich corner of the ternary $CaO–ZrO_2–TiO_2$ composition, if Ca–PSZ is used as the host for alloying Ti^{+4} (14). Thus in order to avoid the formation of (Ca,Ti)–PSZ, the dissolution of Ti^{+4} in ZrO_2 must be faster than Ca^{+2} upon firing. The nucleation and/or growth rate of calzirtite should also be fast enough to bypass the formation of (Ca,Ti)–PSZ.

4.2. Extent of Cation Ordering in Calzirtite

This study showed that the cations Ca, Zr, and Ti were ordered to form a new superstructure of calzirtite, which has been a controversy in the literature as discussed below.

Using single crystals of natural calzirtite, the crystal structure of calzirtite was originally determined by Pyatenko and Pudovkina (15) as an anion-deficient fluorite-related superstructure with ideal fluorite-derived atomic

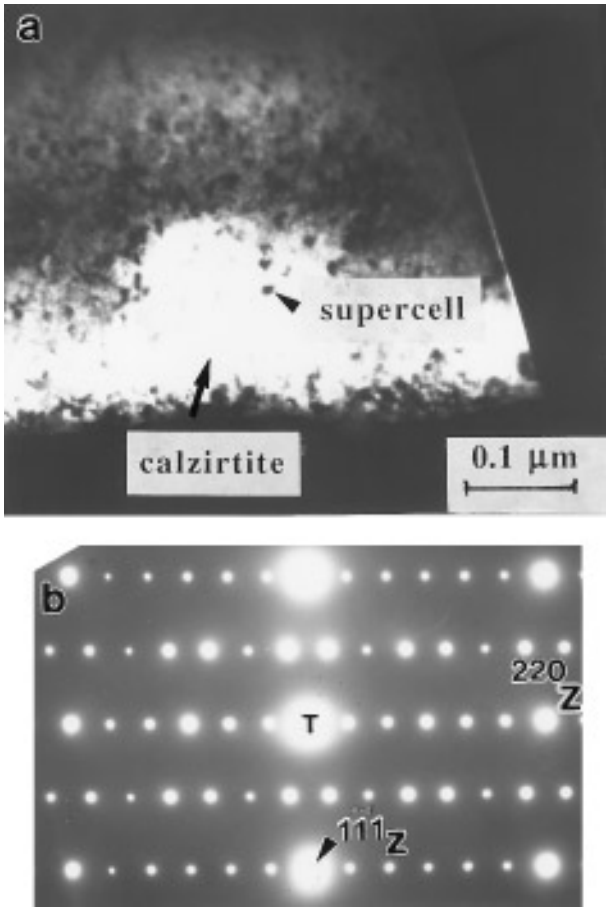

FIG. 8. (a) DFI with (332) spot of calzirtite, i.e., (111) of t-ZrO_2 subcell. The dark areas were nondiffracting and belong to the $6 \times 3 \times 4$ phase. (b) SAD pattern.

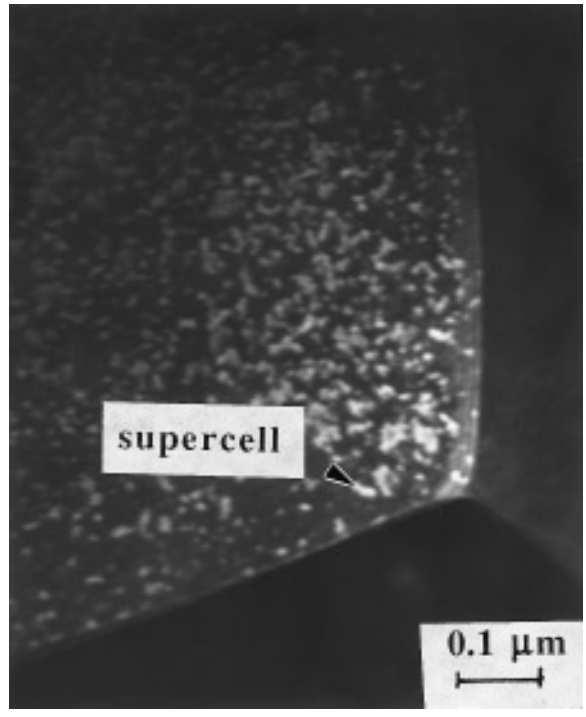

FIG. 9. DFI of the $6 \times 3 \times 4$ supercell (arrow) using the $6 \times 3 \times 4$ spot not superimposing with the calzirtite spots (refer to Fig. 5).

coordinates, fully ordered anion vacancies, and a cation distribution in accord with the O coordination, but they did not refine it. According to Pyatenko (16), the idealized structure containing the cations Ca, Zr, and Ti in a state of complete order would have the composition $Ca_2Zr_5Ti_2O_{16}$. The single phase of this composition synthesized from constituent powders at 1317°C for 2 weeks was studied by Rossell using powder X-ray diffraction and electron diffraction and the refined structure is tetragonal with the space group $I4_1/acd$ (7). The unit cell is a $3 \times 3 \times 2$ array of subcells of defect-fluorite type in which anion vacancies are fully ordered in accord with the choice made by Pyatenko and Pudovkina (15), but the distribution of cations was revised by Rossell (7).

The extent of cation ordering in this revised version is still questioned by Rossell himself (7), in particular the random occupation of one of two closely spaced sites (i.e., the eight-coordinated *M*1 sites which have two positions 0.051 nm apart, as shown schematically in Fig. 12a) by a cation which is unusual in fluorite-related oxides. However, Rossell did not find evidence in electron diffraction patterns for doubling of any cell axes, as might occur if the occupancy of 0.9 Zr and 0.1 Ti in the *M*1 site was ordered.

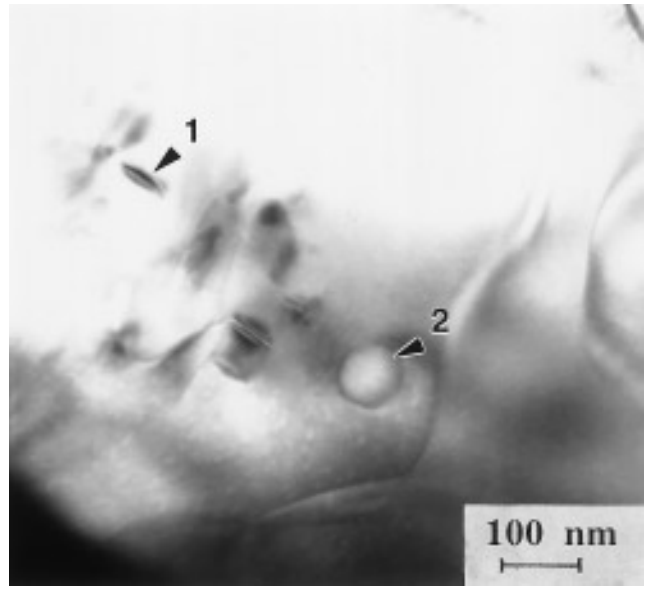

FIG. 10. BFI of disk-like $6 \times 3 \times 4$ phase in two variants.

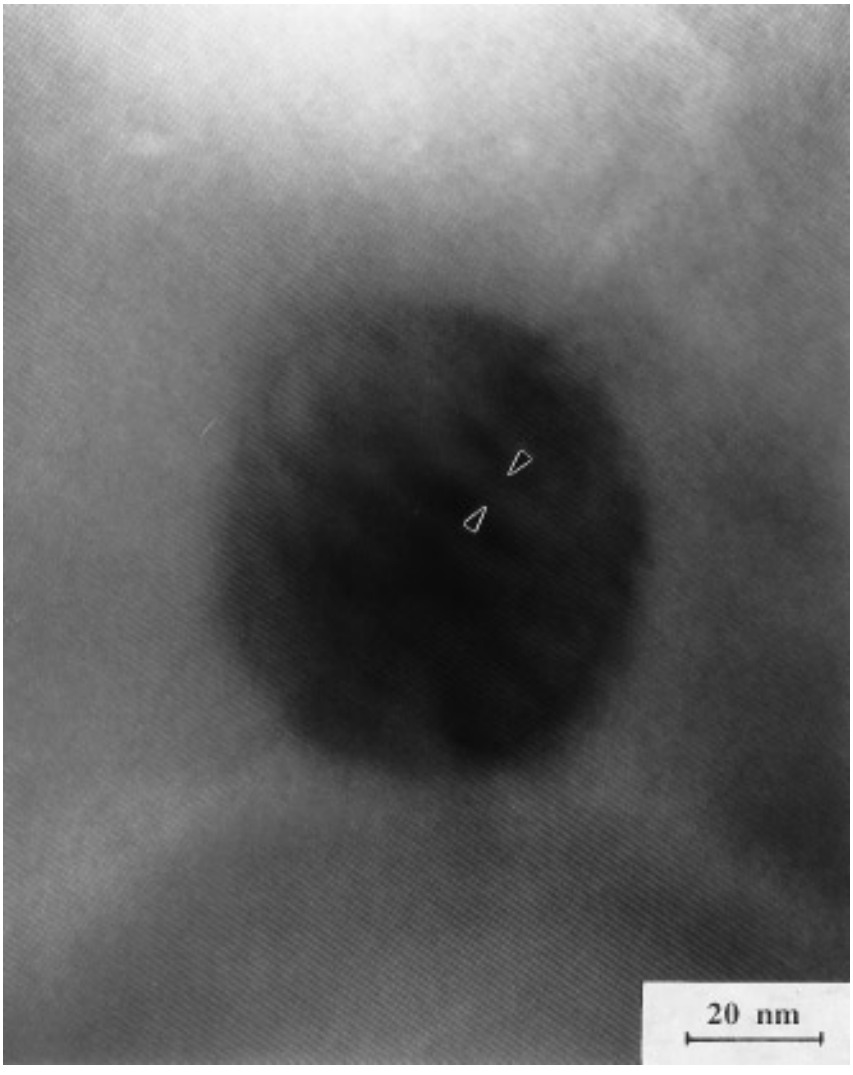

FIG. 11. Lattice image near the [001] zone axis showing that the $6 \times 3 \times 4$ phase is coherent with respect to the calzirtite matrix. Arrows indicate a moiré fringe.

By accident, such evidence was found in this study and the new supercell was indexed tentatively as a $6 \times 3 \times 4$ array of the fluorite subcell. The schematic drawing of the calzirtite and the $6 \times 3 \times 4$ supercell ordered in this manner is shown in Fig. 12b. Critical questions remain as to the effects of annealing time and cooling rate on the extent of cation ordering in calzirtite. Prolonged annealing at suitable temperature is also required to clarify if the coarsened $6 \times 3 \times 4$ supercell forms ordered domains and loses coherency with respect to the calzirtite matrix.

4.3. Implications of Transformation Twin Variants

The twin variants of calzirtite may affect its solid electrolyte applications and may shed light on the formation history of the calzirtite in rocks. In natural occurrences such as carbonatites and alkaline rocks, calzirtite single crystals are tetragonal, prismatic, and bipyramidal without twinning (17), or pseudocubic with orthogonal twinned intergrowths (18). The presence of orthogonal transformation twins implies a c-ZrO_2 and/or PSZ precursor, whereas the absence of twins can be attributed to a lower symmetry precursor, i.e., the t-ZrO_2.

5. CONCLUSIONS

The ZrO_2 (presumably t-symmetry) acted as topotaxial nuclei for the formation of twin-free calzirtite domains and then two variants of a new $6 \times 3 \times 4$ supercell when the constituent oxide powders were subjected to post-sintering dwelling at 1320°C. The microstructures of calzirtite can be used to infer the identity of its precursor, i.e., the symmetry of the ZrO_2 nuclei, and hence may help decipher the

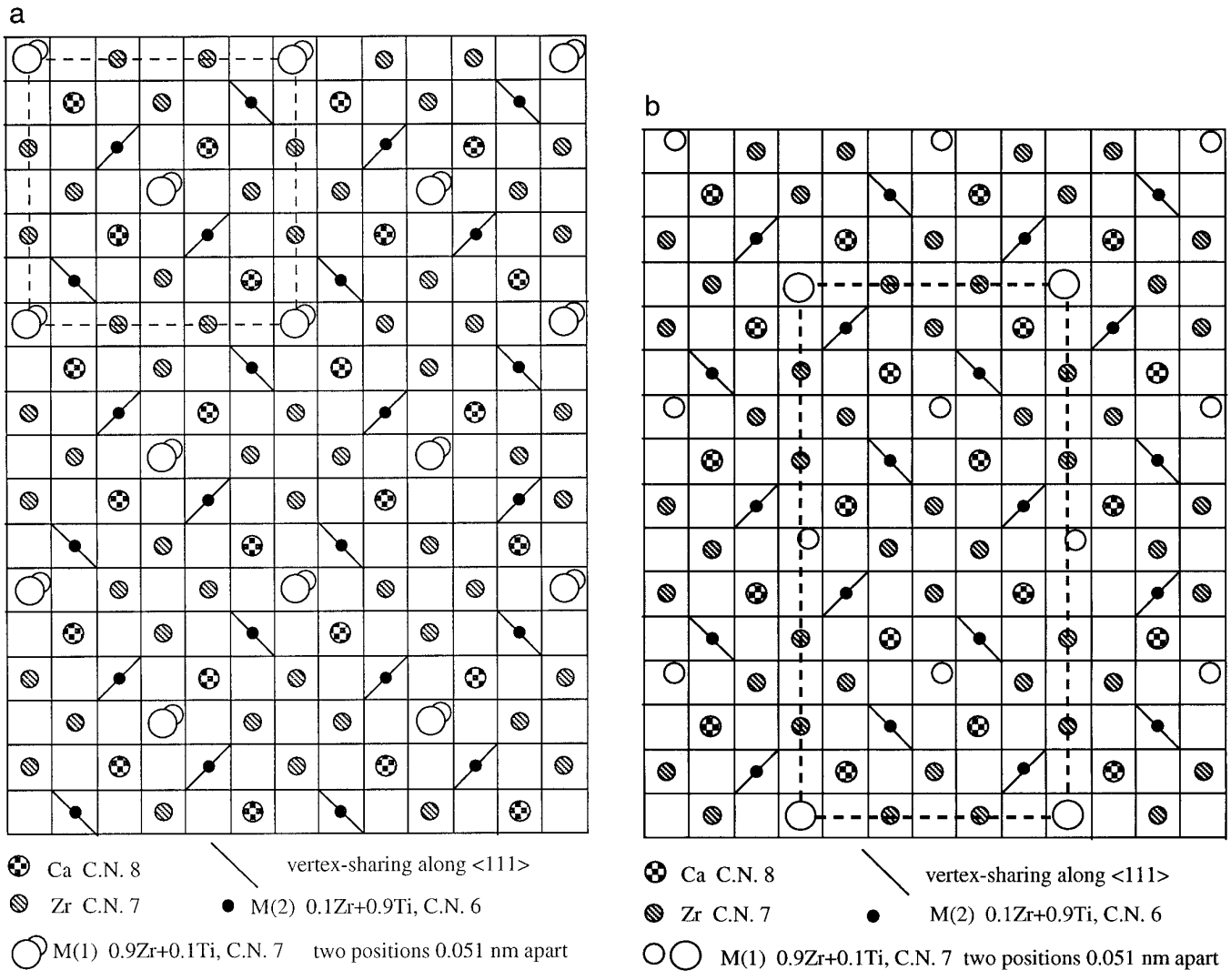

FIG. 12. Lattice sites projected down the *c* axis: (a) the calzirtite ($3 \times 3 \times 2$) subcell after Rossell (7); (b) possible $6 \times 3 \times 4$ supercell of fluorite designated by a dashed line.

metasomatic history of the calzirtite-bearing materials such as the carbonatites and the alkaline rocks.

REFERENCES

1. A. E. Ringwood, S. E. Kesson, N. G. Ware, W. Hibberson, and A. Major, *Nature* **278,** 219 (1979).
2. W. J. Buykx, D. J. Cassidy, C. E. Webb, and J. L. Woolfrey, *Ceram. Bull.* **60,** 1284 (1981).
3. R. A. Penneman and P. G. Eller, *Radiochim. Acta* **32,** 81 (1983).
4. J. M. Reau, J. Portier, A. Levasseur, G. Villeneuve, and M. Pouchard, *Mater. Res. Bull.* **13,** 1415 (1978).
5. M. O. Figueiredo and A. C. D. Santos, *in* "Zirconia '88: Advances in Zirconia Science and Technology," (S. Meriani, and C. Palmonari, Eds.), p. 81. Elsevier Applied Science, London, 1989.
6. P. Shen and Y. Hon, *Mater. Sci. Eng. A* **159,** 267 (1992) and references cited therein.
7. H. I. Rossell, *Acta Crystallogr. B* **38,** 593 (1982) and references cited therein.
8. M. J. Buerger, *J. Chem. Phys.* **15,** 1 (1947).
9. G. Teufer, *Acta Crystallogr.* **15,** 1187 (1962).
10. D. J. Green, R.H.J. Hannink, and M.V. Swain, "Transformation Toughening of Ceramics," CRS, Boca Raton, Florida, 1989.
11. M. J. Bannister and J.M. Barners, *J. Am. Ceram. Soc.* **69,** C269 (1986).
12. C. C. Lin, D. Gan, and P. Shen, *J. Am. Ceram. Soc.* **71,** 624 (1988).
13. E. C. Subbarao, *in* "Advances in Ceramics, Vol. 3, Science and Technology of Zirconia." (A. H. Heuer and L. W. Hobbs, Eds.), pp. 1–24. American Ceramic Society, Columbus, OH, 1981.
14. Y. Hon and P. Shen, *Mater. Sci. Eng. A* **131,** 273 (1991).
15. Yu. A. Pyatenko and Z. V. Pudovkina, *Solv. Phys-Crystallogy* **6,** 155 (1961).
16. Yu. A. Pyatenko, *Izv. Akad. Nauk S.S.S.R. Neorg. Mater.* **7,** 630 (1971).
17. T. B. Zdorik, G. A. Sidorenko, and A. V. Bykova, *Doklady Akad. S.S.S.R.*, **137,** 681 (1961).
18. A. G. Bulakh, G. F. Anastasenko, and L. M. Dakhiya, *Am. Mineral.* **52,** 1880 (1967).